J. Comput. Struct. Eng. Inst. Korea, 27(3)
pp.137~145, June, 2014
http://dx.doi.org/10.7734/COSEIK.2014.27.3.137

pISSN 1229-3059 eISSN 2287-2302
Computational Structural Engineering Institute of Korea

브리징 스케일 기법을 이용한 분자동역학-연속체 연성 시스템의 설계민감도 해석

차 송 현[1] · 하 승 현[2] · 조 선 호[1†]

[1]서울대학교 조선해양공학과 및 아이소-지오메트릭 최적설계 창의연구단, [2]존스홉킨스대학교 토목공학과

Design Sensitivity Analysis of Coupled MD-Continuum Systems Using Bridging Scale Approach

Song-Hyun Cha[1], Seung-Hyun Ha[2] and Seonho Cho[1†]

[1]National Creative Research Initiatives(NCRI) Center for Isogeometric Optimal Design, Department of Naval Architecture and Ocean Engineering, Seoul National University, Seoul, 151-744, Korea
[2]Department of Civil Engineering, Johns Hopkins University, Baltimore, MD 21218, USA

Abstract

We present a design sensitivity analysis(DSA) method for multiscale problems based on bridging scale decomposition. In this paper, we utilize a bridging scale method for the coupled system analysis. Since the analysis of full MD systems requires huge amount of computational costs, a coupled system of MD-level and continuum-level simulation is usually preferred. The information exchange between the MD and continuum levels is taken place at the MD-continuum boundary. In the bridging scale method, a generalized Langevin equation(GLE) is introduced for the reduced MD system and the GLE force using a time history kernel is applied at the boundary atoms in the MD system. Therefore, we can separately analyze the MD and continuum level simulations, which can accelerate the computing process. Once the simulation of coupled problems is successful, the need for the DSA is naturally arising for the optimization of macro-scale design, where the macro scale performance of the system is maximized considering the micro scale effects. The finite difference sensitivity is impractical for the gradient based optimization of large scale problems due to the restriction of computing costs but the analytical sensitivity for the coupled system is always accurate. In this study, we derive the analytical design sensitivity to verify the accuracy and applicability to the design optimization of the coupled system.

Keywords : *design sensitivity analysis, bridging scale method, molecular dynamics, transient dynamic, time history kernel*

1. Introduction

Atom-based molecular dynamics(MD) simulations are very useful in analyzing nano-scale phenomena which cannot be captured in a continuum sense. However, atomistic simulation tools themselves are not sufficient for many of the interesting and fundamental problems that arise in computational mechanics, since the length and time scales used in the MD simulations are still limited. Many multiscale analysis methods have been developed considering both the MD and the continuum analyses to solve the problems such as dislocation (Tadmor and Ortiz, 1996), crack propagation(Park *et al.*, 2005; Farrell *et al.*, 2007), and strain localization(Kadowaki and Liu, 2007) which cannot be solved with only continuum- based concept. The main issue of multiscale problems is how to connect

† Corresponding author:
Tel: +82-02-880-7322; E-mail: secho@snu.ac.kr
Received February 4 2014; Revised March 31 2014;
Accepted May 9 2014

the atom-level simulations to continuum-level. Bridging scale method(BSM)(Wagner and Liu, 2003) is introduced by deriving dynamic multiscale boundary conditions as a damping force using the generalized Langevin equation(GLE)(Adelman and Doll, 1974, 1976). They used the MD in a localized region of interest and the finite element method in a global region by decoupling the fine and coarse scales through a mass-weighted projection. This boundary condition prevents the wave reflection in the fine scale without any handshake or scale down regions.

Mathematically, design sensitivity analysis(DSA) methods are well developed based on continuum mechanics for structural systems(Choi and Kim, 2004). Since the MD is one of transient dynamic problems, DSA for transient dynamic problems is indispensible for the design of nano- and micro-scale problems. However, a huge amount of computation is usually required for the MD simulations since they are transient dynamic problems. For the DSA of MD systems that have many design variables, the computational cost is very expensive. Therefore, an efficient and accurate analytical DSA method is necessary in the problems that include molecular dynamics analysis. However, the DSA in the multiscale analysis is not straightforward, since the sensitivity relationship between the scales is not well known yet. Even though the relations are known, iterative sensitivity computations might be necessary between the fine and coarse scales depending on the multiscale decomposition method. Therefore, for an efficient DSA in the multiscale problems, it is important to choose the decomposition method that could provide fully decoupled scales in the DSA. In this research, we suggest an analytical DSA method using a BSM to avoid the aforementioned difficulties in the multiscale problems including the MD simulations. The BSM defines the fine scale as the solution whose projection onto the coarse scale basis functions vanishes; this implies the orthogonality between the fine and coarse scales. In addition, the projection operator used in the BSM gives fully decoupled multiscale equations, which enables us to avoid iterative computations between the scales and to perform efficient DSA in the multiscale problems.

2. Review of Bridging Scale Method

The bridging scale method was developed to couple atomistic and continuum scale simulation (Wagner and Liu, 2003). The main idea is to decompose the total displacement $\boldsymbol{u}(\boldsymbol{x})$ into coarse and fine scales as

$$\boldsymbol{u}(\boldsymbol{x}) = \bar{\boldsymbol{u}}(\boldsymbol{x}) + \boldsymbol{u}'(\boldsymbol{x}) \tag{1}$$

The coarse scale displacement is defined as

$$\bar{\boldsymbol{u}}(\boldsymbol{x}_\alpha) = \sum_I N_I^\alpha d_I \tag{2}$$

where $N_I^\alpha = N_I(x_\alpha)$ is the shape function of node I at point x_α, and d_I is the FE nodal displacement corresponding to node I. In MD simulation, MD displacement $\boldsymbol{q}$ is regarded as the exact solution. The fine scale displacement is simply that part of the total displacement that the coarse scale cannot represent, and then the error is defined as

$$\sum_\alpha m_a \left(q_\alpha - \sum_I N_I^\alpha w_I \right)^2 \tag{3}$$

which means mass-weighted square of the fine scale, and a temporary nodal solution w_I is determined to minimize the error, which yields

$$\boldsymbol{w} = \boldsymbol{M}^{-1} \boldsymbol{N}^T \boldsymbol{M}_A \boldsymbol{q} \tag{4}$$

where $\boldsymbol{M}_A$ is a diagonal atomic mass matrix, and $\boldsymbol{M} = \boldsymbol{N}^T \boldsymbol{M}_A \boldsymbol{N}$. Then, the fine scale displacement $\boldsymbol{u}'$ is written as

$$\boldsymbol{u}' = \boldsymbol{q} - \boldsymbol{N}\boldsymbol{w} = \boldsymbol{q} - \boldsymbol{P}\boldsymbol{q} \tag{5}$$

where the projection matrix $\boldsymbol{P}$ is defined as

$$P = NM^{-1}N^{T}M_{A} \tag{6}$$

Finally, the total displacement is rewritten as

$$u = Nd + q - Pq = Nd + Qq \tag{7}$$

where the complimentary projector $Q = I - P$.

3. Generalized Langevin Equation

A free vibration equation is generally written as

$$M\ddot{u}(t) + Ku(t) = 0 \tag{8}$$

$u(t)$ is a displacement field at time t, M is a mass matrix, and K is a stiffness matrices. Then we can solve Eq. (8) using the velocity verlet algorithm,

$$u^{n+1} = u^{n} + \dot{u}^{n}\Delta t + \frac{1}{2}\ddot{u}^{n}\Delta t^{2} \tag{9a}$$

$$\dot{u}^{n+\frac{1}{2}} = \dot{u}^{n} + \frac{1}{2}\ddot{u}^{n}\Delta t \tag{9b}$$

$$\ddot{u}^{n+1} = -M^{-1}Ku^{n+1} \tag{9c}$$

$$\dot{u}^{n+1} = \dot{u}^{n+\frac{1}{2}} + \frac{1}{2}\ddot{u}^{n+1}\Delta t \tag{9d}$$

Consider an one-dimensional atomic chain shown in Fig. 1. (a) and (b) show a full MD system and a reduced one, respectively.

For simplicity, M and K are given as

$$M = \begin{bmatrix} m & & & \\ & m & & \\ & & \ddots & \\ & & & m \end{bmatrix}, \quad K = \begin{bmatrix} 2k & -k & & \\ -k & 2k & \ddots & \\ & \ddots & \ddots & \ddots \\ & & \ddots & 2k \end{bmatrix} \tag{10}$$

where $m = k = 1$, and the initial condition is given as Gaussian type distribution as

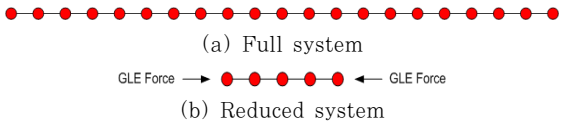

(a) Full system

(b) Reduced system

Fig. 1 One-dimensional atomic chain

$$u(x, t=0) = \begin{cases} \dfrac{e^{-(x/10)^2} - e^{-25}}{1 - e^{-25}} & \text{if } |x| \le 50 \\ 0 & \text{if } |x| > 50 \end{cases} \tag{11}$$

Simulation results for the full MD system are plotted in Fig. 2. It is observed that the initial wave propagates smoothly in both directions.

Assume that displacement $u(t)$ is partitioned into two parts, i.e. u_1 is the solution of interest, whose degrees of freedom will be kept, and u_2 is the solution to be mathematically replaced by boundary forces. In this example, the interface between u_1 and u_2 lies at $x = \pm 80$. Then Eq. (8) is decomposed into those two parts as

$$\begin{pmatrix} \ddot{u}_1 \\ \ddot{u}_2 \end{pmatrix} = -\begin{pmatrix} A_{11} & A_{12} \\ A_{21} & A_{22} \end{pmatrix}\begin{pmatrix} u_1 \\ u_2 \end{pmatrix} \tag{12}$$

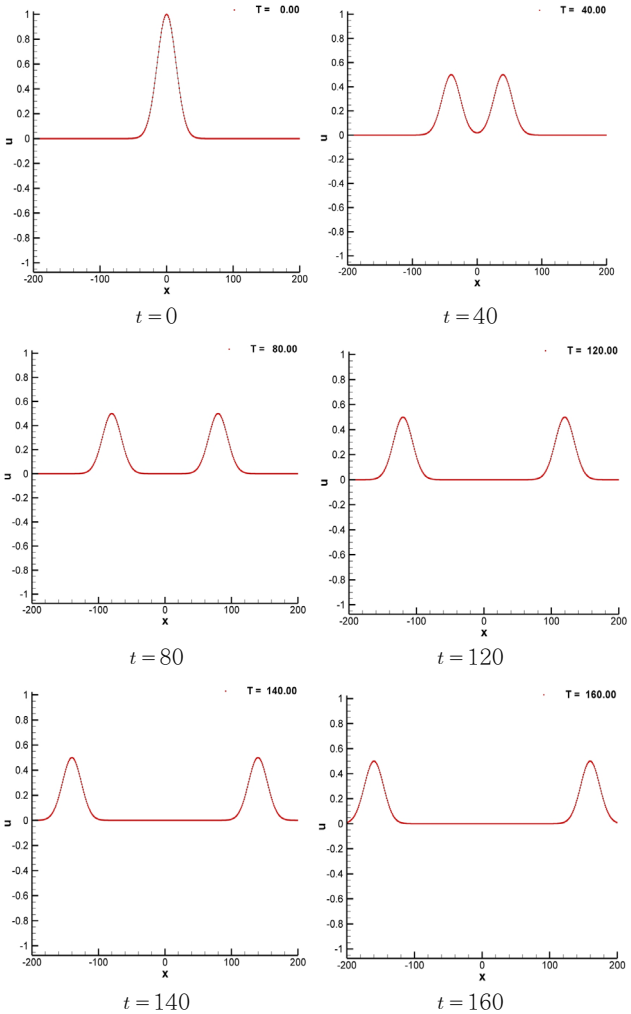

$t = 0$ $t = 40$

$t = 80$ $t = 120$

$t = 140$ $t = 160$

Fig. 2 Wave propagation in Full MD system

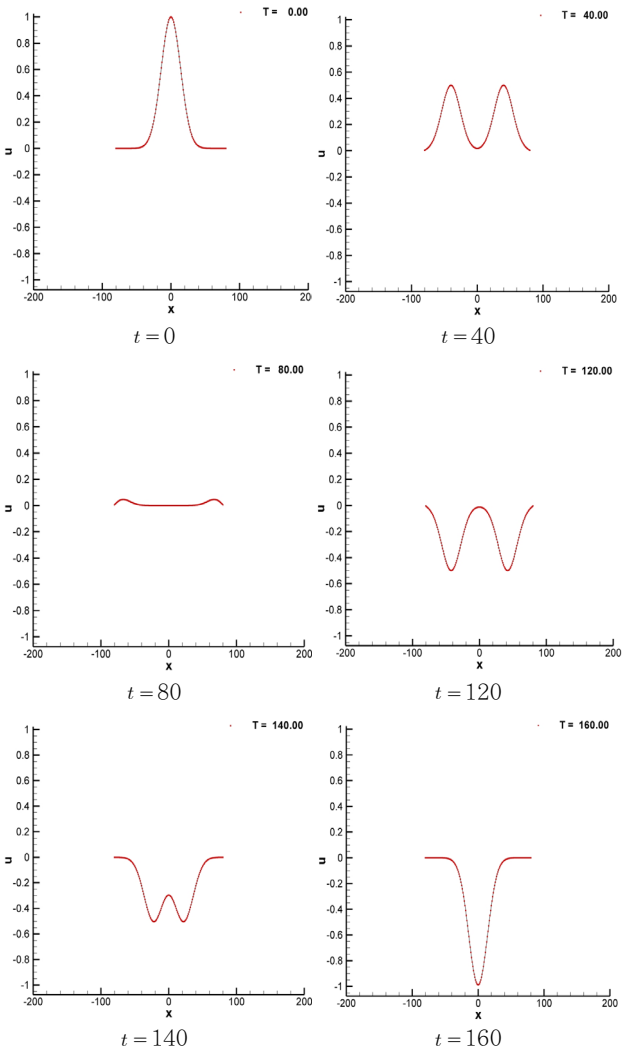

Fig. 3 Wave reflection in Reduced system

where $\boldsymbol{A}=\boldsymbol{M}^{-1}\boldsymbol{K}$. If we merely regard $\boldsymbol{u}_2$ as zero, then we have

$$\ddot{\boldsymbol{u}}_1(t) = -\boldsymbol{A}_{11}\boldsymbol{u}_1(t) \tag{13}$$

When a reduced system is introduced only between $x=\pm 80$ without GLE force, this approach causes an unwanted boundary wave reflection as Fig. 3.

At time $t=160$, the same wave as the initial condition is reflecting with reverse phase. Instead, we introduce generalized Langevin equation to remove boundary reflection. First of all, the degrees of freedom $\boldsymbol{u}_2$ are eliminated by solving Eq. (12) and substituting the result back into the equation for $\boldsymbol{u}_1$.

$$\ddot{\boldsymbol{u}}_2(t) = -\boldsymbol{A}_{21}\boldsymbol{u}_1(t) - \boldsymbol{A}_{22}\boldsymbol{u}_2(t) \tag{14}$$

To obtain $\boldsymbol{u}_2(t)$ explicitly, the Laplace transform is introduced. The Laplace transform of a function $f(t)$, defined for all real numbers $t \geq 0$, is the function $F(s)$ defined by

$$F(s) = L\{f(t)\} = \int_{0^-}^{\infty} e^{-st} f(t)\,dt \tag{15}$$

where the Laplace operator L transforms time domain t into space domain s. The inverse Laplace transform is given by the following complex integral

$$f(t) = L^{-1}\{F(s)\} = \frac{1}{2\pi i}\int_{\gamma-i\cdot\infty}^{\gamma+i\cdot\infty} e^{st} F(s)\,ds \tag{16}$$

where γ is a real number so that the contour path of integration is in the region of convergence of $F(s)$ normally requiring $\gamma > Re(s_p)$ for every singularity s_p of $F(s)$. Using the definition of the Laplace transformation as Eq. (15), the following properties can be derived:

$$L\left\{\frac{df(t)}{dt}\right\} = sF(s) - f(0^-) \tag{17a}$$

$$L\left\{\frac{d^2 f(t)}{dt^2}\right\} = s^2 F(s) - sf(0^-) - \frac{df}{dt}(0^-) \tag{17b}$$

and another useful property of the Laplace transform is the convolution property as

$$L\left\{\int_0^t f(t-\tau)g(\tau)\,d\tau\right\} = F(s)\,G(s) \tag{18}$$

Applying Eq. (17b) into Eq. (14) gives

$$s^2\boldsymbol{U}_2(s) - s\boldsymbol{u}_2(0^-) - \dot{\boldsymbol{u}}_2(0^-) = -\boldsymbol{A}_{21}\boldsymbol{U}_1(s) - \boldsymbol{A}_{22}\boldsymbol{U}_2(s) \tag{19}$$

Rearranging Eq. (19) yields

$$\boldsymbol{U}_2(s) = -\Theta(s)\boldsymbol{A}_{21}\boldsymbol{U}_1(s) + \Theta(s)\left(s\boldsymbol{u}_2(0^-) + \dot{\boldsymbol{u}}_2(0^-)\right) \tag{20}$$

where the matrix $\Theta(s)$ can be written as

$$\Theta(s) = \left(s^2 \boldsymbol{I} + \boldsymbol{A}_{22}\right)^{-1} \tag{21}$$

Taking the inverse Laplace transform on Eq. (20) and using the convolution rule, the equation for $\boldsymbol{u}_2(t)$ is derived as

$$\boldsymbol{u}_2(t) = -\int_0^t \theta(t-\tau)\boldsymbol{A}_{21}\boldsymbol{u}_1(\tau)d\tau + \theta(t)\dot{\boldsymbol{u}}_2(0^-) + \dot{\theta}(t)\boldsymbol{u}_2(0^-) \tag{22}$$

where the time history kernel $\theta(t)$ is

$$\theta(t) = L^{-1}\{\Theta(s)\} \tag{23}$$

For given mass and stiffness matrices $\boldsymbol{M}$ and $\boldsymbol{K}$, $\theta(t)$ is derived analytically(Wagner and Liu, 2003)

$$\theta(t) = 2\omega^{-2}\frac{J_2(2\omega t)}{t} \tag{24}$$

where J_2 is a first-kind second-order Bessel function, and $\omega = \sqrt{k/m}$. Substituting Eq. (22) into Eq. (12) yields the equation for $\boldsymbol{u}_1(t)$

$$\ddot{\boldsymbol{u}}_1(t) = -\boldsymbol{A}_{21}\boldsymbol{u}_1(t) + \int_0^t \boldsymbol{A}_{12}\theta(t-\tau)\boldsymbol{A}_{21}\boldsymbol{u}_1(\tau)d\tau - \boldsymbol{A}_{12}\theta(t)\dot{\boldsymbol{u}}_2(0^-) - \boldsymbol{A}_{12}\dot{\theta}(t)\boldsymbol{u}_2(0^-) \tag{25}$$

The second to fourth terms in Eq. (25) are the GLE forces and prevent boundary reflections. As shown in Fig. 4, the initial wave passes smoothly through the boundary and no reflection happens.

Then, the generalized Langevin equation(GLE) is utilized to simulate a coupled MD-continuum equation. The bridging scale method is applicable to the problems where the MD region is confined to a small portion of the domain, while the continuum region exists in the whole domain. It may be possible to solve the full MD system, but it requires huge amount of computational cost, especially in 2- or 3-dimensional case. The advantage of bridging scale method is that one can precisely solve the specific region of interest using MD simulation, and

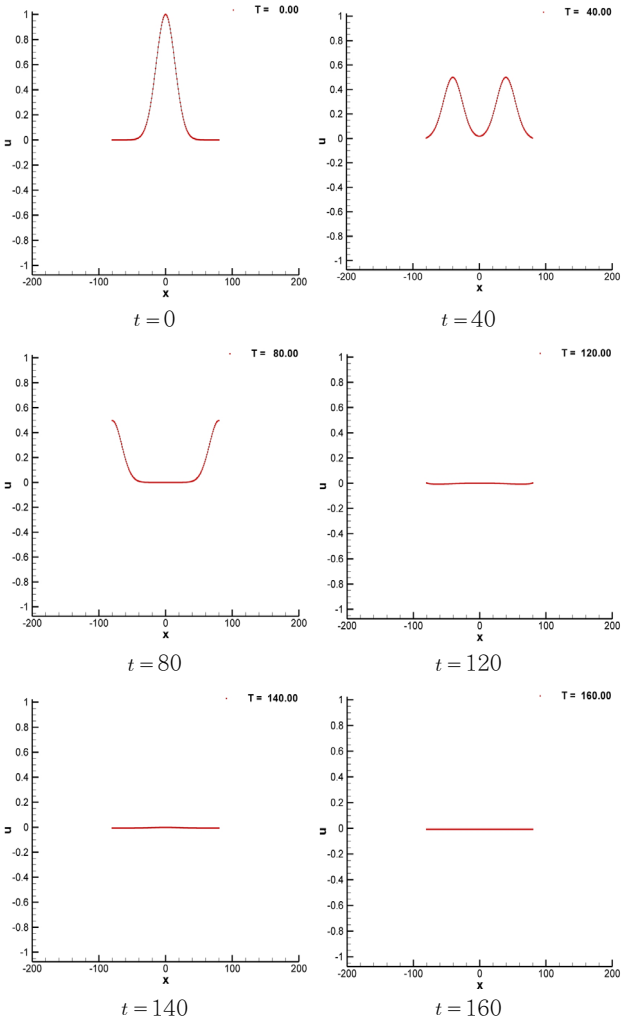

Fig. 4 Reduced system with GLE force

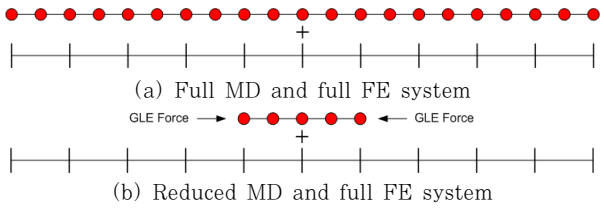

Fig. 5 One-dimensional MD-continuum model

bridge MD solution with continuum solution at the MD-continuum boundary. Also, the fine scale waves in MD region pass the boundary smoothly into continuum region by GLE force.

Consider one-dimensional MD-continuum coupled simulation(Park and Liu, 2004) as shown in Fig. 5. The entire domain is $-200 \le x \le 200$, and the MD particles lie at $-80 \le x \le 80$.

In brief, the coupled MD/FE equations of motion are described as

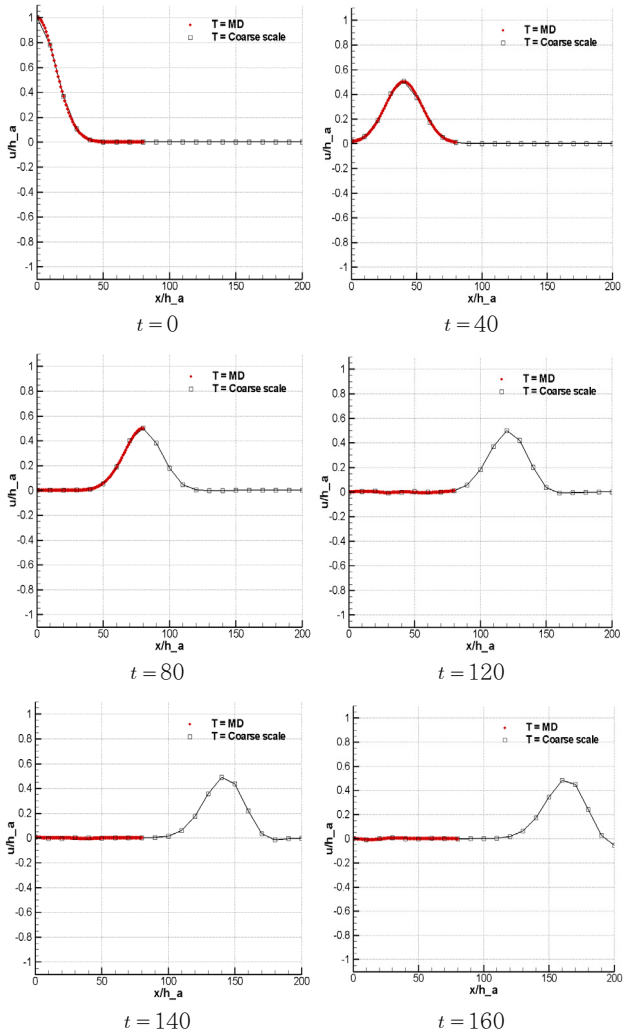

Fig. 6 BSM with GLE force at MD-continuum boundary

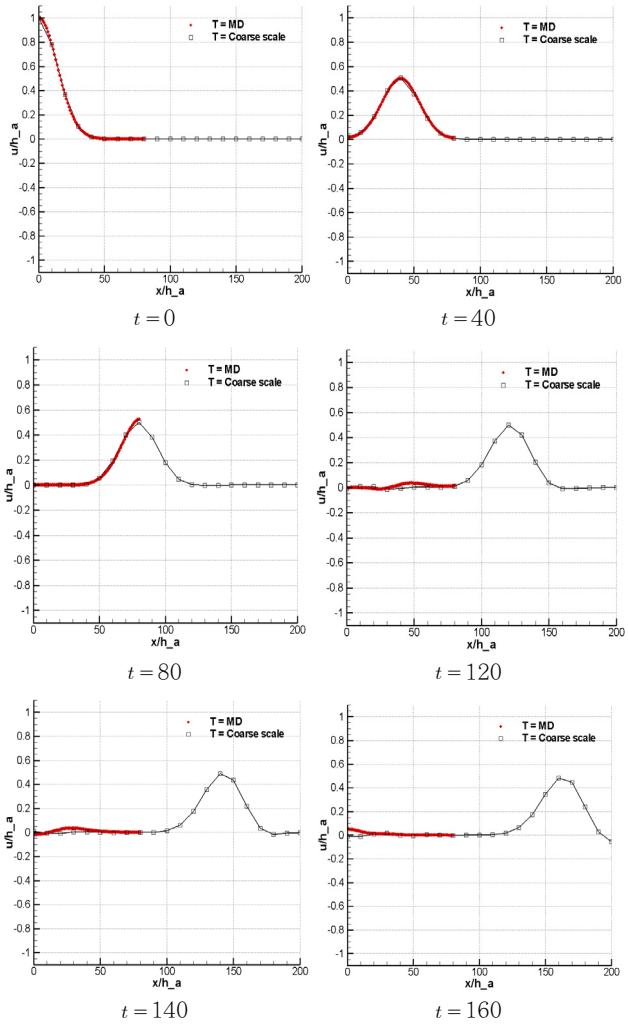

Fig. 7 BSM with boundary velocity approach

$$q_1(t) = M_{A1}^{-1} f_1(\bar{u}, u'_1, u'_2 = 0) + \int_0^t \theta(t-\tau)\left(q_1(\tau) - \bar{u}_1(\tau)\right)d\tau \quad (26)$$

$$M\ddot{d} = N^T f(u) = N^T f(Nd + Qq) \quad (27)$$

In Fig. 6 and 7, the solid and void dots denote the positions of MD particles and FE nodal points, respectively. From the initial condition, a wave is propagating in both directions. Due to symmetry, the solution at $x \geq 0$ is plotted in all the figures. In Fig. 6, GLE force is applied at MD-continuum boundary and the initial wave passes out of the MD region smoothly without any boundary reflections.

However, if the boundary condition is simply applied by setting the MD velocity at the boundary equal to the coarse scale velocity, the fine scale waves cannot pass through the MD-continuum boundary and undesirable wave reflections occur at the boundary as shown in Fig. 7.

4. Design Sensitivity Analysis

Assume that $u_2(t)$ has zero initial condition as

$$u_2(0^-) = \dot{u}_2(0^-) = 0 \quad (28)$$

Then, Eq. (25) is rewritten as

$$\ddot{u}_1(t) = -A_{11}u_1(t) + \int_0^t A_{12}\theta(t-\tau)A_{21}u_1(\tau)d\tau \quad (29)$$

4.1 Perturbation of A_{11} by 0.1%

Table 1 Design sensitivity agreement at $x=0$

Time t	Finite difference sensitivity	Analytical sensitivity	Agreement (%)
50	-5.98328E-05	-6.00210E-05	99.69
100	1.55272E-07	1.53035E-07	101.46
150	8.59221E-04	8.56186E-04	100.35
200	5.61980E-05	5.61980E-05	99.22
250	3.72665E-05	3.72915E-05	99.93
300	3.36549E-05	3.36158E-05	100.12
350	3.45926E-06	3.43558E-06	100.69
400	1.70420E-06	1.69541E-06	100.52

The design sensitivity equation for $\boldsymbol{u}_1(t)$ is obtained from the derivative of Eq. (29) with respect to stiffness k as

$$\frac{\partial \ddot{\boldsymbol{u}}_1(t)}{\partial k} = -\frac{\partial \boldsymbol{A}_{11}}{\partial k}\boldsymbol{u}_1(t) - \boldsymbol{A}_{11}\frac{\partial \boldsymbol{u}_1(t)}{\partial k} + \int_0^t \boldsymbol{A}_{12}\theta(t-\tau)\boldsymbol{A}_{21}\frac{\partial \boldsymbol{u}_1(\tau)}{\partial k}d\tau \tag{30}$$

Using velocity verlet algorithm, the displacement sensitivity $\frac{\partial \boldsymbol{u}_1(t)}{\partial k}$ is updated. The derivative $\frac{\partial \boldsymbol{A}_{11}(t)}{\partial k}$ is easily obtainable, and $\boldsymbol{u}_1(t)$ is already available from the dynamic solution of Eq. (8). The accuracy of design sensitivity of displacement is verified in Table 1. For each time step t, the analytic sensitivity is compared with the finite difference sensitivity. In the last column, very good agreement is observed at every time step.

4.2 Perturbation of all A by 0.1%

The design sensitivity equation for $\boldsymbol{u}_1(t)$ is obtained from the derivative of Eq. (29). Unlike Eq. (30), there are more design dependent terms as

$$\begin{aligned}\frac{\partial \ddot{\boldsymbol{u}}_1(t)}{\partial k} = &-\frac{\partial \boldsymbol{A}_{11}}{\partial k}\boldsymbol{u}_1(t) - \boldsymbol{A}_{11}\frac{\partial \boldsymbol{u}_1(t)}{\partial k} \\ &+ \int_0^t \boldsymbol{A}_{12}\theta(t-\tau)\boldsymbol{A}_{21}\frac{\partial \boldsymbol{u}_1(\tau)}{\partial k}d\tau \\ &+ \int_0^t \frac{\partial \boldsymbol{A}_{12}}{\partial k}\theta(t-\tau)\boldsymbol{A}_{21}\boldsymbol{u}_1(\tau)d\tau \\ &+ \int_0^t \boldsymbol{A}_{12}\theta(t-\tau)\frac{\partial \boldsymbol{A}_{21}}{\partial k}\boldsymbol{u}_1(\tau)d\tau\end{aligned} \tag{31}$$

Table 2 Design sensitivity agreement at $x=0$

Time t	Finite difference sensitivity	Analytical sensitivity	Agreement (%)
50	-5.98328E-05	-6.00210E-05	99.69
100	-1.13985E-08	-1.12662E-08	101.17
150	-1.38233E-04	-1.37916E-04	100.23
200	-7.19341E-05	-7.19751E-05	99.94
250	-6.47973E-05	-6.48062E-05	99.99
300	-6.08876E-05	-6.09023E-05	99.98
350	-5.08988E-05	-5.09237E-05	99.95
400	-4.41505E-05	-4.41762E-05	99.94

The derivatives $\frac{\partial \boldsymbol{A}_{11}(t)}{\partial k}$, $\frac{\partial \boldsymbol{A}_{12}(t)}{\partial k}$ and $\frac{\partial \boldsymbol{A}_{21}(t)}{\partial k}$ are easily obtainable, and $\boldsymbol{u}_1(t)$ is already available from the dynamic solution of Eq. (8). Using the relation

$$J_\nu = \frac{1}{2}(J_{\nu-1} - J_{\nu+1}) \tag{32}$$

the derivative of time history kernel $\theta(t)$ is derived as

$$\begin{aligned}\frac{\partial \theta(t)}{\partial k} &= -2\frac{m}{k^2}\cdot\frac{J_2(2\omega t)}{t} \\ &\quad + 2\frac{m}{k}\cdot\frac{J_1(2\omega t) - J_3(2\omega t)}{2t}\cdot\left(2\cdot\frac{1}{2\sqrt{mk}}t\right) \\ &= -\frac{2}{\omega^2 k}\cdot\frac{J_2(2\omega t)}{t} + \frac{1}{\omega k}\{J_1(2\omega t) - J_3(2\omega t)\}\end{aligned} \tag{33}$$

The accuracy of design sensitivity of displacement is also verified in Table 2. For each time step t, the analytic sensitivity is compared to the finite difference sensitivity. In the last column, good agreement is observed at every time step.

5. Conclusions

A multi-scale DSA method is developed using a bridging scale approach. To avoid any iterative computations between the scales, we use a fully decoupled equation for each scale in original response

as well as sensitivity analyses. Through a GLE, a locally confined MD region instead of whole MD system is considered for the fine scale solution whereas a FE analysis for the coarse scale solution is performed on the whole region. The efficiency of the developed method is achieved due to the fully decoupled multi-scale equations in these scales, which are derived using identical mass-weighted projection in the response analysis. Numerical implementations demonstrate the accuracy of the developed DSA method for various design variables. The developed method turns out to work very well for any design variable in both scales.

Acknowledgement

This work was supported by the National Research Foundation of Korea(NRF) grant funded by the Korea government(MSIP)(No. 2010-0018282). The support is gratefully acknowledged. The authors would also like to thank Ms. Inyoung Cho at Korea University for editing assistance.

Reference

Adelman, S.A., Doll, J.D. (1974) Generalized Langevin Equation Approach for Atom/Solid-Surface Scattering: Collinear atom/harmonic Chain, *The Journal of Chemical Physics*, 61(10), pp.4242~4245.

Adelman, S.A., Doll, J.D. (1976) Generalized Langevin Equation Approach for Atom/Solid-Surface Scattering: General Formulation for Classical Scattering off Harmonic Solids, *The Journal of Chemical Physics*, 64(6), pp.2375~2388.

Cho, S., Choi, K.K. (2000) Design Sensitivity Analysis and Optimization of Non-Linear Transient Dynamics Part I: sizing design, *International Journal for Numerical Methods in Engineering*, 48, pp.351~373.

Choi, K.K., Kim, N.H. (2004) Structural Sensitivity Analysis and Optimization: Volume 1, Linear Systems & Volume 2, Nonlinear Systems and Applications, Springer, New York.

Farrell, D.E., Park, H.S., Liu, W.K. (2007) Implementation Aspects of the Bridging Scale Method and Application to Intersonic Crack Propagation, *International Journal for Numerical Methods in Engineering*, 71, pp.583~605.

Kadowaki, H., Liu, W.K. (2007) Bridging Multi-Scale Method for Localization Problems, *Computer Methods in Applied Mechanics and Engineering*, 193, pp.1733~1772.

Kim, M.G., Ha, S.H., Cho, S. (2012) Level Set Based Topological Shape Optimization of Hyper-Elastic Nonlinear Structures Using Topological Derivatives, *J. Comput. Struct. Eng. Inst. Korea*, 25(6), pp.559~567.

Park, H.S. Liu, W.K. (2004) An Introduction and Tutorial on Multiple-Scale Analysis in Solids, *Computer Methods in Applied Mechanics and Engineering*, 193, pp.1733~1772.

Park, H.S., Karpov, E.G., Klein, P.A., Liu, W.K. (2005) Three-Dimensional Bridging Scale Analysis of Dynamic Fracture, *Journal of Computational Physics*, 207, pp.588~609.

Tadmor, E.B., Ortiz, M., Phillips, R. (1996) Quasi Continuum Analysis of Defects in Solids, *Philosophical Magazine*, 73(6), pp.1529~1563.

Tang, S., Hou, T.Y.. Liu, W.K. (2006) A Mathematical Framework of the Bridging Scale Method, *International Journal for Numerical Methods in Engineering*, 65, pp.1688~1713.

Wagner, G.J., Liu, W.K. (2003) Coupling of Atomistic and Continuum Simulations Using a Bridging Scale Decomposition, *Journal of Computational Physics*, 190, pp.249~274.

요 지

본 논문에서는 브리징 스케일 분해를 기반으로 멀티스케일 문제에 대한 설계민감도 해석법을 개발하였다. 나노 기술의 급속한 발전으로 인해 나노 수준의 해석의 필요성이 지속적으로 증가하고 있다. 최근 분자동역학과 연속체역학의 연성문제에서 많은 해석 방법들이 개발되었다. 본 논문에서는 연성시스템 해석을 위해 브리징 스케일 기법을 사용한다. 전체 영역의 분자동역학 시스템의 해석은 많은 양의 계산 비용이 들기때문에 분자동역학과 연속체 시뮬레이션의 연성시스템을 선호한다. 분자동역학과 연속체 수준 사이의 정보 교환은 분자동역학과 연속체의 경계에서 일어난다. 브리징 스케일 법에서 일반화된 랑지벵 방정식은 축소된 영역의 분자동역학 시스템 해석을 위하여 요구되고, 시간이력 커널을 사용하여 구한 GLE 힘은 분자동역학 시스템에서 경계에 있는 원자들에 작용한다. 그러므로 분자동역학과 연속체 수준의 시뮬레이션을 분리해서 해석할 수 있으며 계산 과정을 가속시킬 수 있다. 연성문제의 시뮬레이션 이후에는 설계의 최적화를 위해 설계민감도 해석의 필요성이 자연스럽게 나타나며 전체 시스템의 성능은 나노 스케일의 효과를 고려해서 최적화된다. 설계구배 기반 최적화에서 설계민감도가 요구되지만 유한차분법으로 구한 민감도는 문제가 대형화될 때 계산비용의 제한때문에 비실용적이나 해석적 설계민감도는 효율적인 강점을 갖는다. 본 연구에서는 연성된 분자동역학-연속체 멀티스케일 문제에서 해석적 설계민감도를 유도하여 정확성과 향후 최적설계로의 활용 가능성을 확인하였다.

핵심용어 : 설계민감도 해석, 브리징 스케일 기법, 분자동역학, 과도 동역학, 시간이력 커널